Small-Signal Analysis of High-Temperature Stable 1550nm High-Speed VCSELs

M. Müller,[1] T. Gründl,[1] M. Horn,[1] R. D. Nagel,[1] W. Wiedmeier,[1]
E. Rönneberg,[2] G. Böhm,[1] and M.-C. Amann[1]

[1] *Walter Schottky Institut, Technische Universität München, Am Coulombwall 3, 85748 Garching, Germany, mueller@wsi.tum.de*
[2] *VERTILAS GmbH, Lichtenbergstr. 8, 85748 Garching, Germany*

ABSTRACT
We present 1.55µm Buried Tunnel Junction (BTJ) Short-Cavity (SC) VCSELs for application in access networks. A detailed analysis of the temperature-dependent static and small-signal modulation performance of these devices is given. Record-high modulation bandwidth beyond 17 GHz at 20°C and 11 GHz at 80°C are reported and discussed with respect to the proper electro-optical and thermal design.

Keywords: Vertical-Cavity Surface-Emitting Laser (VCSEL), semiconductor lasers, direct modulation, frequency response, InP, optical communication, access networks.

1. INTRODUCTION

The unprecedented growth of bandwidth demand in telecommunications which is especially driven by the increasing data-traffic in local and access networks, necessitates the development of low-cost, high-speed optical links [1]. As an essential photonic component of such links, cheap laser-diodes featuring high modulation-bandwidths, reasonable output-power with at the same time low power consumption, and emission in the near-infrared are required. For short-range transmission distances (10 - 100 m) Vertical-Cavity Surface-Emitting Lasers (VCSELs) with bandwidths exceeding 20 GHz and emission around 850 nm serve these needs [2,3]. For the transmission ranges of fibre-to-the-home (FTTH) and passive optical networks (PONs), great efforts in developing high-speed VCSELs for the 1.3 µm and 1.55 µm wavebands have been made allowing direct modulation schemes up to 15 GHz and 22 Gbit/s, respectively [4-7].

In this work, we present a detailed analysis of the temperature-dependent modulation performance of 1.55 µm high-speed VCSELs. These devices operate at an extremely low power budget facilitating record-high modulation bandwidths both at room-temperature and elevated temperatures up to 80°C. As will be shown, the presented VCSELs are excellent candidates for uncooled high-speed operation over the entire temperature range from 20°C to 80°C without adjustment of the bias-current. In order to understand these excellent electrical, optical, and thermal device properties, the paper is organized as follows. Section one gives a detailed description of the various design elements of the Short-Cavity (SC) VCSEL, motivating the outstanding high-speed and high-temperature operation of the devices. The second part discusses the static device performance with special emphasis on the power budget and thermal device properties. In the third section conducted S-Parameter measurements are presented. Curve-fitting of the measured modulation response allows the extraction of characteristic parameters like resonance-frequency, *D*- and *K*-factor for different temperatures. The obtained results are discussed with respect to the proper choice of mode-gain offset, the reduced photonic lifetime as well as device parasitics. Suggestions for further design-improvements are inferred.

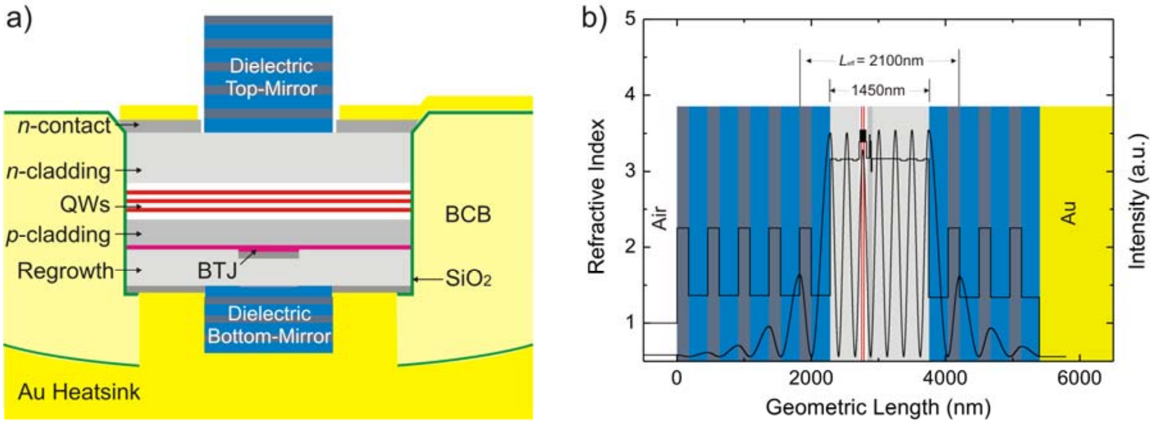

Figure 1.a Schematic cross section of a BTJ SC-VCSEL.
b) Refractive index profile and longitudinal field square of SC-VCSEL

2. Device Structure

The InP-based high-speed SC-VCSELs discussed in this paper come with a novel short cavity design depicted in Fig. 1.a as introduced in detail in [4]. The active region of these devices contains seven highly compressively strained AlGaInAs/InGaAs quantum wells yielding higher (differential) gain and, therefore, enhancing the relaxation-resonance frequency f_R. Current confinement is achieved by a BTJ placed in the node of the electrical field to reduce absorption losses (Fig. 1.b). Likewise, all current-guiding layers are modulation doped to reduce free carrier absorption, internal losses as well as internal heating. Moreover, these negative effects are further reduced by the application of an extremely short cavity yielding less internal losses and improved heat-sinking. Furthermore, by introducing two dielectric DBRs with high refractive index contrast among individual layer pairs (see Fig. 1.b), an effective cavity length of only 2.3 µm can be achieved, leading to reduced photon lifetimes and high modulation bandwidths [4]. In order to reduce device-parasitics under RF-modulation, benzocyclobutene (BCB) is used as low ε-dielectric passivation material reducing the parasitic capacitance of the coplanar contact-pads [8]. Together with the excellent intrinsic modulations behaviour this allows record high modulation bandwidths as will be presented in section 4.

3. Static Device Performance

All presented results belong to a typical single-mode SC-device with a current aperture of 5 µm and an effective cavity-length of 2.3 µm. Figure 2.a plots the voltage and output-power versus current characteristics (*L-I-V*) at various heat-sink temperatures. The maximum optical output power is 3 mW at 20°C and still exceeds 1.3 mW at 80°C. Threshold currents are as low as 0.7 mA and 1.9 mA, respectively. As depicted in Fig. 2.b, the maximum wall plug efficiency (WPE) ranges from 12% at 80°C up to 20% at room-temperature. Driving the device in the current range of maximum WPE around 4 mA, allows device operation with a total power budget below 5 mW and optical output-powers between 0.5 mW at 80°C and 1mW at 20°C as indicated by the shaded areas in Fig. 2.a,b. As will be shown in section 4 these devices can be modulated at 10 GHz at such low bias-currents over the entire temperature range, making them a power-efficient answer to the needs of customer units, where uncooled high-speed operation is favoured.

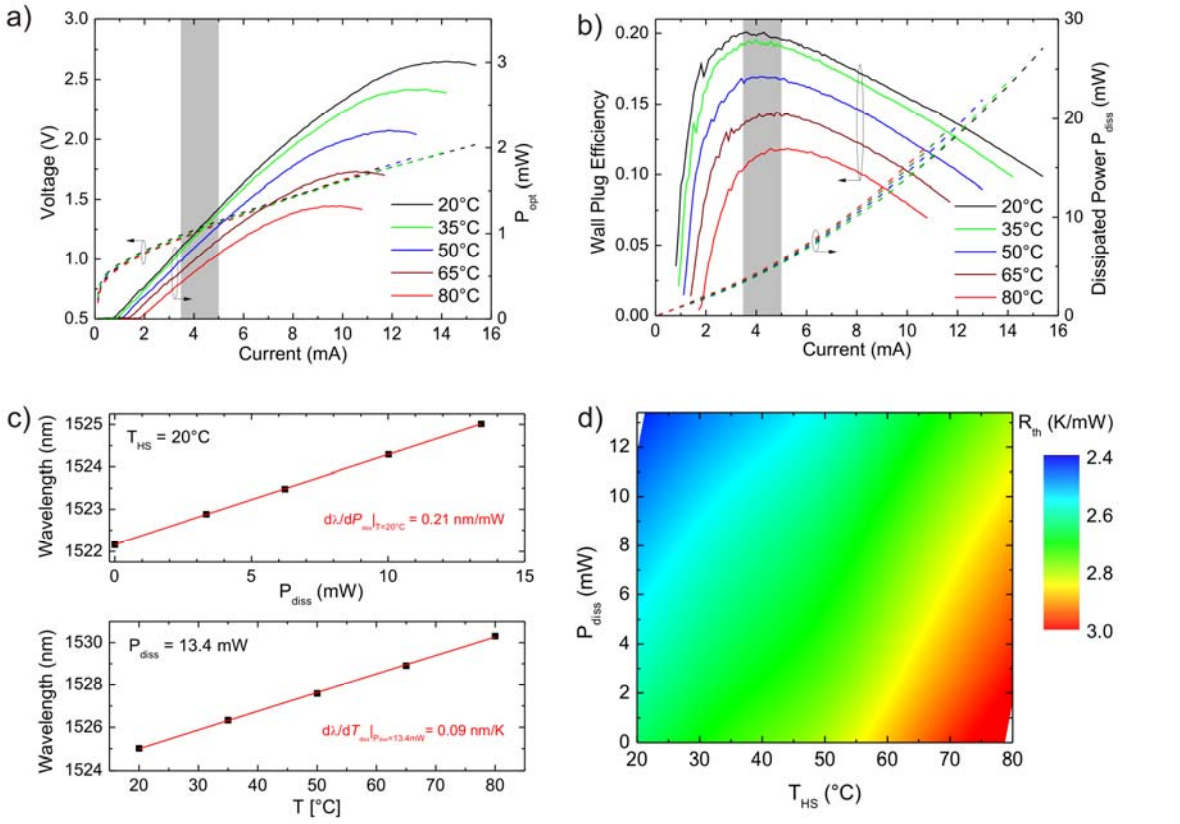

Figure 2. Static device performance of a single-mode SC VCSEL with 5 µm active diameter a) L-I-V curves at different temperatures b)Wall-plug efficiency and dissipated power at various temperatures c) Current- and thermal-tunability d) Thermal resistance as a function of dissipated power and heat-sink temperature.

In order to conduct the additionally dissipated power plotted in Fig. 2.b, a proper heat-management is required. As a figure of merit, the thermal resistance R_{th} is calculated from the ratio of the power tuning coefficient $d\lambda \,/\, dP_{diss}\,|_{\,T_{HS}}$ and the thermal tuning coefficient $d\lambda \,/\, dT\,|_{\,P_{diss}}$ determined from Fig. 2.c for a heat-sink temperature of 20°C and a dissipated power of 13.4 mW, respectively. Since the heat-conductivity of the InP-cladding layers decreases with increasing temperature, the thermal tuning coefficient increases for larger dissipated powers, and the current tuning coefficient inclines with rising heat-sink temperatures. This behaviour explains the mapping of the thermal resistance in Fig. 2.d, where R_{th} varies between 2.4 and 3.0 K/mW confirming excellent heat-management even at elevated temperatures.

4. Small-Signal Modulation Response

S-parameter measurements were performed with the test system described in [4]. The RF input power was chosen -20 dBm. Figures 4.a and 4.b plot the small signal modulation responses for various currents at 20°C and 80°C, respectively. At room-temperature maximum modulation bandwidths exceed 17 GHz with an extremely flat frequency response. As the comparison of Fig. 3.a and 3.b suggests, the VCSELs can be operated at a constant bias-current of 4 mA and a modulation bandwidths of at least 10 GHz over the entire temperature range from 20°C to 80°C redundantising passive cooling and current control. Since these devices were originally designed for room-temperature operation with a mode-gain offset of only 25 nm at 20°C, the temperature-stable modulation behaviour can be mainly attributed to the excellent heat-sinking.

As shown in [9] the 3-pole filter function *H(f)* accurately describes the VCSEL modulation-response.

$$H(f) = \eta_{d,L}\eta_{d,PD} \cdot \frac{f_R^2}{f_R^2 + j\dfrac{\gamma}{2\pi}f - f^2} \cdot \frac{1}{1 + j\dfrac{f}{f_P}}$$

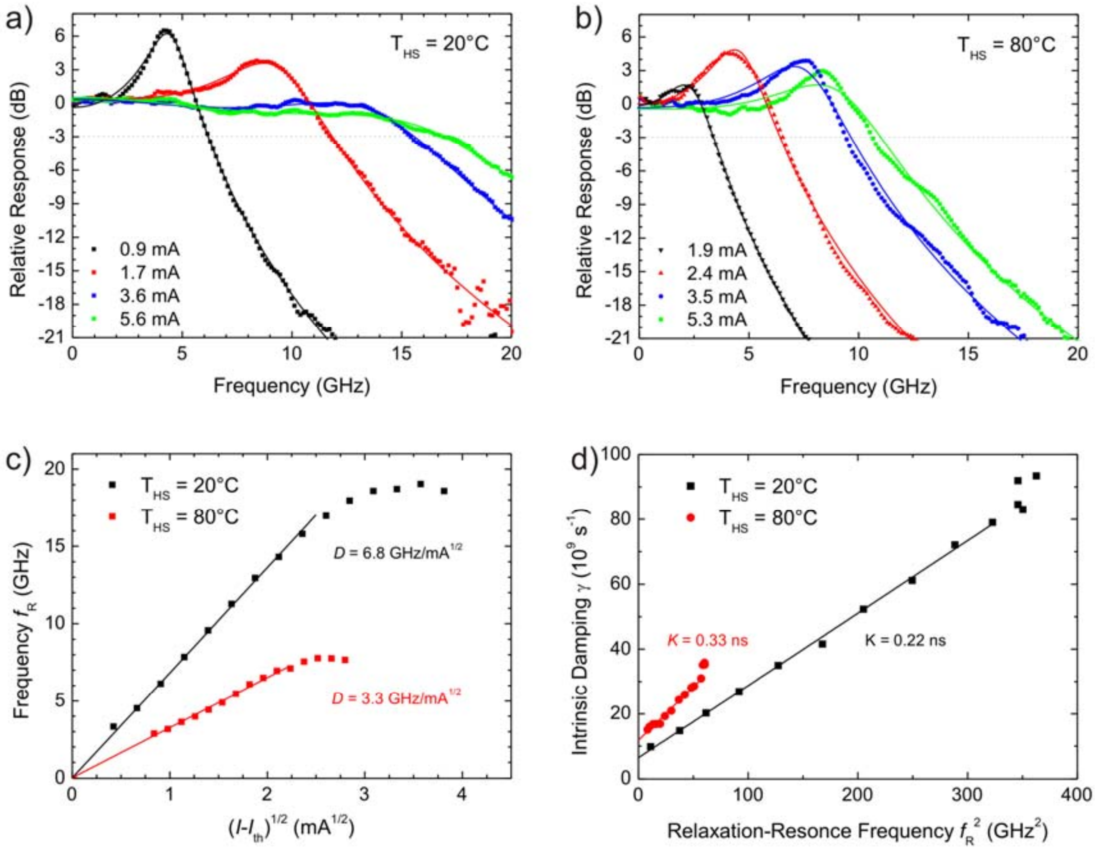

Figure 3. Small-signal modulation response of a single-mode SC-VCSEL with 5 µm active diameter a,b) Scatters depict the relative response S_{21} for various currents at 20°C and 80°C, respectively; solid lines are fits to the data c) Extracted relaxation-resonance frequencies and D-factors at 20°C and 80°C d) Intrinsic damping versus relaxation-resonance frequency squared; extracted K-factors at 20°C and 80°C are indicated.

Thereby, $\eta_{d,L}$, $\eta_{d,PD}$ are the differential quantum efficiencies of the laser and detector, $\gamma = \gamma_0 + K f_R^2$ the damping rate, γ_0 the damping offset, K the K-factor, f_P the parasitic cut-off frequency, and f_R the relaxation-resonance frequency. From the fit of $|H(f)|^2$ to the data in Fig. 4.a,b, f_R is extracted and depicted in Fig. 4.c as a function of injected current above threshold for operation at both 20°C and 80°C. In the low current regime, where self-heating is small, a D-factor of 6.8 GHz/mA$^{1/2}$ is extracted at 20°C from the slope of f_R, indicating high differential gain a and small photon lifetime τ_p since $f_R \propto D \propto \sqrt{a/\tau_p} \propto \sqrt{a/L_{eff}}$. The high values of f_R up to 19 GHz can be attributed to the extremely short effective cavity length and the therefore reduced photon lifetime. At 80°C the rather low D-factor of 3.3 GHz/mA$^{1/2}$ suffers from the thermal degradation of the differential gain, which for future designs can be compensated by an increased mode-gain offset. From a maximum f_R of 7.5 GHz a thermal damping limit of $f_{3dB,\ thermal}$ = 11.5 GHz follows which is in agreement with Fig. 3.b. The plot of the intrinsic damping rate as a function of relaxation-resonance frequency squared in Fig. 3.d, allows the extraction of the K-factor which is 0.22 ns at 20°C and 0.33 ns at 80°C again confirming the effect of a shorter cavity and the thermal degradation of the differential gain since $K = 4\pi\tau_p(1+\Gamma a_P/a)$, where a a_P is the differential photon gain and Γ the confinement factor. Therefore, neither at 20°C nor at 80°C the intrinsic damping is limiting the modulation bandwidth since determined damping frequencies $f_{3dB,\ damping}$ are 40 GHz and 27 GHz, respectively. The extracted parasitic cut-off frequency f_P from the fit of $|H(f)|^2$ to Fig. 3.a,b is 7.0 ± 0.5 GHz yielding a parasitic damping limit of 24 GHz. Since the thermal damping limit is 29 GHz at 20°C the modulation bandwidth at this temperature is most likely limited by the device parasitics. Despite the deconvolution of laser- and the calibrated photodiode-response ($f_{3dB,PD}$ = 15 GHz), the extracted laser-response in Fig. 3.a might even underestimate the actual modulation bandwidth of the VCSELs for high bias-currents.

5. CONCLUSION

InP-based BTJ-VCSELs with novel short cavity design and record-high modulation bandwidth beyond 17 GHz at 20°C and 11 GHz at 80°C have been presented. A shorter effective cavity length strongly pushes the modulation bandwidth and reduces intrinsic damping due to shorter photon lifetime as reflected by high D- and low K-factors. The low thermal resistance mirrors the excellent heat-management of these devices and allows the temperature stable modulation at 10 GHz at a record-low power-budget of only 5 mW over the entire temperature range from 20°C to 80°C.

Moreover, the presented short-cavity devices enable bit-rates of 25 Gbit/s over fiber at room-temperature as confirmed by large signal measurements [10]. Therefore, parallel approaches of 4x25 Gbit/s lanes are suitable for the application in 100G Ethernet solutions.

REFERENCES

[1] E. Kapon, A. Sirbu: Long-wavelength VCSEL - Power-efficient answer, *Nature Photonics*, vol. 3. pp. 27-29, Jan. 2009.

[2] P. Westbergh, et al.: High-Speed, Low-Current-Density 850 nm VCSELs, *IEEE Journal of Selected Topics in Quantum Electronics,* vol. 15, no. 3, pp. 694-703, May/June 2009.

[3] R. H. Johnson, D. M. Kuchta: 30 Gb/s directly modulated 850 nm datacom VCSELs, *CLEO 2008*, San Jose, CA, paper CPDB2, 2008.

[4] M. Müller, et al.: Short-Cavity Long-Wavelength VCSELs with Modulation Bandwidths in Excess of 15 GHz, *IEEE Photonics Technology Letters*, vol. 21, no. 21, pp. 1615 - 1617, Nov. 2009.

[5] W. Hofmann, M. Müller, A. Nadtochiy, C. Meltzer, A. Mutig, G. Böhm, J. Rosskopf, D. Bimberg, M.-C. Amann, and C. Chang-Hasnain, “22-Gb/s Long Wavelength VCSELs,” *Opt. Express*, vol. 17, no. 20, pp. 17547-17554, Sept. 2009.

[6] A. Gatto, et al.: 1.3 µm VCSEL Transmission Performance up to12.5 Gb/s for Metro Access Networks, *IEEE Photonics Technology Letters*, vol. 21, no. 12, June 2009.

[7] Y. Onishi, et al.: Long-Wavelength GaInNAs Vertical-Cavity Surface-Emitting Laser With Buried Tunnel Junction, *IEEE Journal of Selected Topics in Quantum Electronics*, vol. 15, no. 3, May/June 2009.

[8] M. Müller, et al.: Low-Parasitics 1.55 µm VCSELs with Modulation Bandwidths beyond 17 GHz, *CLEO 2010*, San Jose, CA, paper CME5, May 2010.

[9] M.-C. Amann, W. Hofmann: InP-based long-wavelength VCSELs and VCSEL arrays, *IEEE Journal of Selected Topics in Quantum Electronics*, vol. 15, no. 3, pp. 861-868, Sept. 2009.

[10] M. Mueller, et al.: 1.55 µm High-Speed VCSELs Enabling Error-Free Fiber-Transmission up to 25 Gbit/s, *Proceedings of International Semiconductor Laser Conference (ISLC)*, September 26-30, Kyoto, 2010.